

# Secure Multi-Path Routing with All-or-Nothing Transform for Network-on-Chip Architectures

Hansika Weerasena, Matthew Randall and Prabhat Mishra

Department of Computer & Information Science & Engineering

University of Florida, Gainesville, Florida, USA

**Abstract**—Ensuring Network-on-Chip (NoC) security is crucial to design trustworthy NoC-based System-on-Chip (SoC) architectures. While there are various threats that exploit on-chip communication vulnerabilities, eavesdropping attacks via malicious nodes are among the most common and stealthy. Although encryption can secure packets for confidentiality, it may introduce unacceptable overhead for resource-constrained SoCs. In this paper, we propose a lightweight confidentiality-preserving framework that utilizes a quasi-group based All-Or-Nothing Transform (AONT) combined with secure multi-path routing in NoC-based SoCs. By applying AONT to each packet and distributing its transformed blocks across multiple non-overlapping routes, we ensure that no intermediate router can reconstruct the original data without all blocks. Extensive experimental evaluation demonstrates that our method effectively mitigates eavesdropping attacks by malicious routers with negligible area and performance overhead. Our results also reveal that AONT-based multi-path routing can provide 7.3x reduction in overhead compared to traditional encryption for securing against eavesdropping attacks.

## I. INTRODUCTION

Modern heterogeneous Systems-on-Chip (SoCs) and Multi-Processor SoCs (MPSoCs) now integrate hundreds of Intellectual Property (IP) cores to meet the growing application demands. Network-on-Chip (NoC) enables scalable, low-latency, high-bandwidth and efficient communication among these cores through an interconnected set of routers. Since the NoC facilitates communication between all IP cores, it presents an ideal threat vector—a goldmine for attackers to exploit and pose a significant security challenge. The integration of third-party IPs due to market timing constraints and reliance on untrusted foundries increase the risk of hardware Trojans and compromised routers, which can undermine system confidentiality, integrity, or availability.

NoC security vulnerabilities across different security goals have been extensively studied [1]. Figure 1 shows an illustrative example of eavesdropping attack, which is one of the most common and stealthy threats to on-chip communication. It is a passive attack where a compromised router silently monitors flits as they traverse the network, potentially leaking sensitive information such as encryption keys, inference results, or memory addresses. Traditional defenses, including cryptographic encryption (e.g., AES-CTR), provide strong confidentiality guarantees but may introduce significant area, performance, and energy overhead, making them impractical for many SoC designs. These limitations highlight the need for a lightweight solution that can provide strong protection

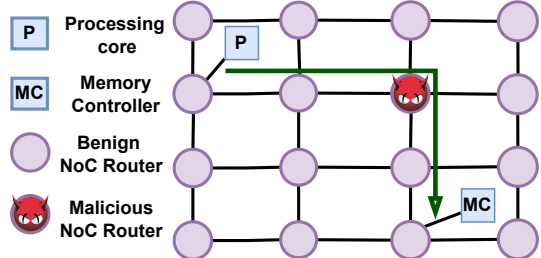


Fig. 1: An example of eavesdropping attack in a 4x4 mesh NoC. A malicious router can eavesdrop on communications between a processing core (P) and a directory controller (DC).

against passive threats like eavesdropping. We propose a lightweight confidentiality-preserving framework for on-chip communication, making it well-suited for resource-constrained SoCs. This paper makes the following contributions.

- We develop a lightweight All-Or-Nothing Transform (AONT) that splits a message into multiple blocks, all of which are needed to reconstruct the original.
- We propose a non-overlapping multipath routing strategy for mesh NoCs to distribute transformed blocks.
- We evaluate our approach across diverse scenarios, demonstrating strong confidentiality with minimal area and performance overhead.

While chaffing and winnowing-based AONT has been used for securing NoC [2], our work introduces a synergetic integration of AONT with disjoint multipath routing, eliminating redundant traffic and achieving superior performance.

## II. THREAT MODEL

In NoC-based MPSoCs, the NoC plays a key role in communicating cache coherence messages for directory-based protocols, such as MESI or MOESI. On a local cache miss, the core issues a control packet (e.g., load or store request) to the shared L2 or last-level cache (LLC), which may forward the request to memory if the data is not cached. Once the data is located, either from the LLC or main memory, a response is sent back to the requesting core as a data packet. This round-trip communication takes place entirely over the NoC, often passing through multiple intermediate routers. Here, we assume a widely adopted mesh NoC topology. Figure 1 illustrates an eavesdropping attack in a 4x4 mesh NoC, where a single malicious router is strategically placed to eavesdrop. A single malicious router is widely used as a realistic threat model since it would be hard to detect during design time due

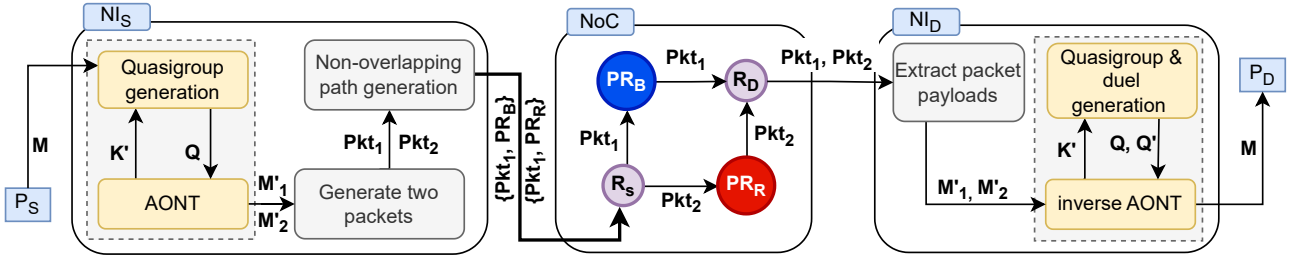


Fig. 2: Overview of the proposed all-or-nothing transform (AONT)-based multi-path routing framework.

to its minimal area and power footprint. The malicious router can intercept in-transit data packets between legitimate nodes. This allows it to extract sensitive information, such as cryptographic keys, proprietary deep learning model parameters, or private user data originating from memory, posing a serious confidentiality threat in safety- and security-critical systems.

### III. SECURE MULTI-PATH ROUTING WITH AONT

To enhance confidentiality in on-chip communication, we implement a lightweight multi-path routing mechanism combined with an All-Or-Nothing Transform (AONT) in mesh NoCs. Our approach consists of two main components: (1) a quasigroup-based AONT and (2) non-overlapping multi-path routing. Figure 2 illustrates the process when a payload  $M$  is sent from source  $P_S$  to destination  $P_D$ . The source network interface ( $NI_S$ ) first generates a quasigroup  $Q$ . The AONT uses  $Q$  to transform  $M$  into two pseudo-messages,  $M'_1$  and  $M'_2$ , which serve as the payloads for packets  $Pkt_1$  and  $Pkt_2$ . Non-overlapping path generation selects two pivot routers ( $PR_B$  and  $PR_R$ );  $Pkt_1$  is routed via  $PR_B$  and  $Pkt_2$  via  $PR_R$ , before both reach the destination router ( $R_D$ ). Non-overlapping paths ensure that no single malicious router can access all AONT blocks, thereby guaranteeing complete confidentiality with no possibility of even partial data leakage. At the destination, the network interface extracts the payloads of the two packets,  $M'_1$  and  $M'_2$ . Finally, the inverse AONT uses quasigroup and the dual to recover the original message  $M$ . The rest of this section describes three important steps in our methodology: AONT and packetization, multi-path routing, and packet reassembly and inverse AONT.

#### A. All or Nothing Transformation and Packetization

AONT is a cryptographic primitive that transforms a message into multiple blocks such that all blocks are needed to recover the original message, any missing block prevents even partial message recovery. Algorithm 1 describes the AONT using quasigroups and packet generation. The message is reformatted to support arithmetic operations in base  $n$  (line 2). Here, the message is divided into  $s$  blocks  $B_1, B_2, \dots, B_s$ , where each block  $B_i = (h_{i1}, h_{i2}, \dots, h_{in})$  contains  $n$  elements. Each element  $h_{ij}$  is represented in base  $n$  using  $\log_2 n$  bits. For instance, when  $n = 4$ ,  $(01)_2$  maps to 1 and  $(11)_2$  to 3. For less computationally demanding base conversion,  $n$  is chosen as a power of two, which motivates using a Fermat prime for  $p$ . Fermat primes, of the form  $2^{2^z} + 1$ , where  $z$  is an integer, enables efficient modular arithmetic with base- $n$  values. The call to Algorithm 2 constructs the quasigroup

#### Algorithm 1 AONT and Packetization

```

1: function AONT_AND_PACKET( $M$ )
2:    $M \leftarrow B_1 \parallel \dots \parallel B_s$  where  $B_i = (h_{i1}, \dots, h_{in})$ 
3:    $K' \leftarrow$  random permutation
4:    $\langle Q, \bullet \rangle, - \leftarrow Quasi(K')$ 
5:    $l_1 \leftarrow k_1, l_2 \leftarrow k_2 \bullet l_1, \dots, l_n \leftarrow k_n \bullet l_{n-1}$  and  $l \leftarrow l_n$ 
6:   for  $i = 1$  to  $s$  do
7:      $I(i) \leftarrow$  base- $n$  representation of  $i$  with  $|I(i)| = n$ 
8:      $R(i) \leftarrow (r_{i1}, \dots, r_{in})$  where  $r_{in} \leftarrow l \bullet i_{in}, r_{in-1} \leftarrow r_{in} \bullet i_{in-1}, \dots, r_{i1} \leftarrow r_{i2} \bullet i_{i1}$ 
9:      $B'_i \leftarrow (h'_{i1}, \dots, h'_{in})$  where  $h'_{ij} \leftarrow r_{ij} \bullet h_{ij}$ 
10:     $C_1 \leftarrow B'_1$ 
11:    for  $i = 2$  to  $s$  do
12:       $C_i \leftarrow C_{i-1} * B_i$ 
13:       $B'_{s+1} \leftarrow C_s * K'$ 
14:       $M'_1, M'_2 \leftarrow B'_1 \parallel \dots \parallel B'_{s/2}, B'_{s/2+1} \parallel \dots \parallel B'_{s+1}$ 
15:       $Pkt_1, Pkt_2 \leftarrow head(Pkt_1) \parallel M'_1, head(Pkt_2) \parallel M'_2$ 
16:   return  $Pkt_1, Pkt_2$ 

```

$\langle Q, \bullet \rangle$  using the randomly generated key  $K'$  (line 4). A finite quasigroup of order  $n$  defines a binary operation  $\bullet$  over a set  $Q$  such that, for any  $a, b \in Q$ , the equations  $a \bullet x = b$  and  $y \bullet a = b$  have unique solutions for  $x$  and  $y$ . The *leader*  $l$  is derived by iteratively applying  $\bullet$  over elements of  $K'$  (line 5).

Lines 6–9 transform each message block  $B_i$  into a pseudo-message block  $B'_i$  as follows: line 7 represents the integer  $i$  in base- $n$  as a length- $n$  vector  $I(i)$  (e.g.,  $i = 1 = (0001)_4$  in base-4 becomes  $(4, 4, 4, 1)$ , where the character 4 denotes 0). In line 8, an intermediate block  $R(i)$  is computed by applying the binary operator  $\bullet$  to the elements of  $I(i)$ , using the leader  $l$  as the  $n^{\text{th}}$  element. Finally, line 9 produces the pseudo-block  $B'_i$  by element-wise application of  $\bullet$  between  $B_i$  and  $R(i)$ . Lines 10–13 compute the final pseudo-block  $B'_{s+1}$  by iteratively combining blocks  $C_i = C_{i-1} * B_i$ , where  $C_1 = B'_1$ , and  $*$  is defined as  $(a_i \cdot b_i) \bmod p$  for each element. Then, the pseudo message  $M'_1$  is formed by concatenating  $B'_1$  to  $B'_{s/2}$  and  $M'_2$  by concatenating the rest of AONT blocks (line 14). Finally,  $Pkt_1$  is created by using  $M'_1$  as payload and  $Pkt_2$  is created by using  $M'_2$  as payload (line 15). *head()* function will generate headers for respective packets.

1) *Quasigroups Generation:* Our approach adopts the quasigroup generation technique proposed by Marnes et al. [3], as it enables a fast and randomized construction process (Algorithm 2). A Latin Square (LS) is an  $n \times n$  matrix over  $n$  symbols, where each symbol appears exactly once in every row

and column. The multiplication table of a quasigroup of order  $n$  is a Latin Square of the same size. In our case,  $n = p - 1$ , where  $p$  is a prime. The first row of the LS is initialized as a random permutation and provided as input to the algorithm (line 2). Each element in the  $i$ -th row, for  $i = 2, \dots, n$ , is computed using the formula  $(i \times q_{1j}) \bmod p$  (line 5). The resulting LS is used in the AONT transformation. Algorithm 2 also generates the dual of the quasigroup simultaneously, although only the inverse AONT at the receiver side requires it. For each element  $q_{ij}$  in row  $i$  and column  $j$ , the corresponding dual element  $q'_{ix}$  is set to  $j$ , where  $x = q_{ij}$  (lines 6 and 7).

#### Algorithm 2 Generating Quasigroup with Dual

```

1: function Quasi( $K'$ )
2:    $q_{11} \parallel q_{12} \parallel \dots \parallel q_{1n} \leftarrow K'$ 
3:   for  $i = 1$  to  $n$  do
4:     for  $j = 1$  to  $n$  do
5:        $q_{ij} \leftarrow (i \times q_{1j}) \bmod p$ 
6:        $x \leftarrow q_{ij}$ 
7:        $q'_{ix} \leftarrow j$ 
8:    $\langle Q, \bullet \rangle, \langle Q, \circ \rangle \leftarrow \text{LS of } q_{ij}, \text{ LS of } q'_{ix}$ 
9:   return  $\langle Q, \bullet \rangle, \langle Q, \circ \rangle$ 

```

#### B. Non-overlapping Path Generation

$Pkt_1$  and  $Pkt_2$  are routed along two disjoint paths to ensure that no single router can intercept all AONT blocks. NoC is divided into two regions, blue and red, based on the source's position relative to the destination. The blue region is selected according to the rules in Table I; the remaining area forms the red region. Figure 3 illustrates the case when the destination lies bottom-right of the source. Red region uses XY routing (X first, then Y) and blue uses YX routing (Y first, then X). Note that virtual channels are equally divided between XY and YX to avoid deadlocks. A random pivot router ( $PR$ ) is selected from each region. The source sends one part of the message to the red  $PR$  and the other to the blue  $PR$ , and both then forward their parts to the actual destination. To support two-hop routing via intermediate nodes, each packet ( $Pkt_1$  and  $Pkt_2$ ) includes the pivot router and the final destination ( $fin\_id$ ) as metadata in packet header. At the pivot router, the packet header is updated to route to the final destination.

TABLE I: Blue Region Selection Rules

Case/Scenario	Blue Region Square
dest is top-right of src	Above src and left of dest
dest is bottom-right of src	Below src and left of dest
dest is top-left of src	Above src and right of dest
dest is bottom-left of src	Below src and right of dest

Two special cases arise when the source and destination lie on the same row or column. In such cases, the NoC is divided into top-bottom or left-right halves, respectively, and each packet is routed through a pivot router in a different half. However, using the default routing strategy may lead to path overlaps in these scenarios. To address this, we introduce an optional *flip\_route* flag that allows the blue path to flip its routing strategy (from YX to XY) at the blue pivot router.

This flip is triggered when the source and destination lie on the same row or column, where spatial constraints can cause potential path overlap. Flipping the blue path's routing strategy ensures disjoint routes in these two special cases. This method guarantees spatial separation of the two paths, ensuring confidentiality against a eavesdropping malicious router.

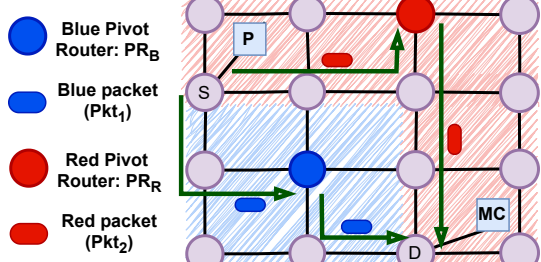


Fig. 3: NoC is divided into two regions: blue and red

#### C. Packet Reassembly and Inverse AONT

Algorithm 3 outlines the packet reassembly and inverse AONT process. At the destination node, the payloads of  $Pkt_1$  and  $Pkt_2$  are first reassembled based on their packet sequence numbers and their payload is extracted (line 2). Once combined, the inverse AONT is applied to reconstruct the original message with the following key differences from the AONT process. First, in line 6, the key  $K'$  is recovered via element-wise division of  $C_s$  by  $B'_{s+1}$  using the relation  $(a \cdot k') \bmod p = m' \iff a/m' = k'$ . Then, in line 7, the quasigroup along with its corresponding dual are reconstructed. Finally, in line 12, the original message blocks are recovered from the pseudo blocks using the dual operator  $\circ$  of  $\bullet$ . Here, a dual binary operator  $\circ$  can be defined for a given binary operator  $\bullet$  over the set  $Q$  such that  $a \circ b = c$  if and only if  $a \bullet c = b$ . This relationship defines a new finite quasigroup  $\langle Q, \circ \rangle$ , which is the dual of  $\langle Q, \bullet \rangle$ . The following identities hold:  $a \circ (a \bullet b) = b$  and  $a \bullet (a \circ b) = b$ .

#### Algorithm 3 Packet reassembly and Inverse AONT

```

1: function REASSEMBLE_AND_AONT $^{-1}$ ( $Pkt_1, Pkt_2$ )
2:    $M'_1, M'_2 \leftarrow \text{extract payload from } Pkt_1 \text{ and } Pkt_2$ 
3:    $B'_1 \parallel \dots \parallel B'_s \leftarrow M'_1 \parallel M'_2 \text{ where } B'_i = (h'_{i1}, \dots, h'_{in})$ 
4:    $C_1 \leftarrow B'_1$ 
5:   for  $i = 2$  to  $s$  do
6:      $C_i \leftarrow C_{i-1} * B'_i$ 
7:    $K' \leftarrow C_s / B'_{s+1}$ 
8:    $\langle Q, \bullet \rangle, \langle Q, \circ \rangle \leftarrow \text{Quasi}(K')$ 
9:    $l_1 \leftarrow k_1, l_2 \leftarrow k_2 \bullet l_1, \dots, l_n \leftarrow k_n \bullet l_{n-1} \text{ and } l \leftarrow l_n$ 
10:  for  $i = 1$  to  $s$  do
11:     $I(i) \leftarrow \text{base-}n \text{ representation of } i \text{ with } |I(i)| = n$ 
12:     $R(i) \leftarrow (r_{i1}, \dots, r_{in}) \text{ where } e_{in} \leftarrow l \bullet i_{in}, r_{in-1} \leftarrow r_{in} \bullet i_{in-1}, \dots, r_{i1} \leftarrow r_{i2} \bullet i_{i1}$ 
13:     $B(i) \leftarrow (h_{i1}, \dots, h_{in}) \text{ where } h_{ij} \leftarrow r_{ij} \circ h'_{ij}$ 
14:   $M \leftarrow B_1 \parallel B_2 \parallel \dots \parallel B_{s+1}$ 
15:  return  $M$ 

```

#### IV. EXPERIMENTS

We used a combined setup with cycle-accurate gem5 [4] and Noxim [5]. Full-system simulations in gem5 generated network traces using seven SPLASH-2 [6] and PARSEC [7] benchmarks, which were then used for trace-driven simulations in Noxim. The simulated system features a two-level MESI cache coherence protocol, x86 cores operating at 2GHz, and an 8x8 mesh interconnect with 64 nodes. Each core has 32KB private L1 I/D caches, and all cores share a 512KB L2 cache. We extended Noxim to support our proposed security mechanism by integrating AONT, inverse AONT and multi-path route generation at the NIs, and destination swap support at routers. We compare against AES-128, a widely adopted standard, as lightweight ciphers like Hummingbird lack standardization and have known vulnerabilities. Since our design supports parallel AONT transformation, we compare it against AES-128 in parallel CTR mode to ensure a fair comparison. The evaluation includes three scenarios: (1) No Security, (2) Our Proposed Method, and (3) AES-128 in CTR mode.

##### A. Experimental Results

Table II presents the average delay across seven benchmarks on an 8x8 NoC for three configurations: no security, AES-128, and our proposed method. For each benchmark, we conducted experiments over 20 random application-to-core mappings, and the reported values reflect the average delay across these runs. Compared to the no-security baseline (12.9 cycles), AES-128 increases average delay by over 20x (261.5 cycles), while our method incurs only a 2.8x increase (35.9 cycles). This demonstrates that our AONT-based approach provides strong confidentiality with significant (7.3x) reduction in performance overhead compared to traditional encryption. We also compared our approach with the chaffing and winnowing-based AONT scheme from [2]; our approach achieves superior performance with 83.9% reduction in average packet latency. This is because the chaffing process significantly increase the packet sizes ( $\approx 4x$ ) due to multiple counters and authentication tags.

TABLE II: Performance comparison for 8x8 mesh NoC

Benchmark	Delay: No Security		Delay: AES-128		Delay: Proposed	
	Avg	Max	Avg	Max	Avg	Max
FFT	13.2	31	259.1	630	36.5	97
OCEAN	13.1	33	258.3	626	35.1	95
RADIX	14.1	33	259.5	628	34.2	99
FMM	10.9	33	266.9	630	35.5	101
LU	13.6	31	258.2	628	37.0	99
BARNEs	11.2	31	270.5	630	36.2	101
black	13.9	31	257.9	626	36.6	99
Average	12.9	33	261.5	630	35.9	101

Table III shows the average delay for experiments where two benchmarks were run concurrently on an 8x8 NoC. Similarly to the single-benchmark case, we averaged results over 20 random application mappings. If we focus on table entry (e.g., *FFT + 1*), each main benchmark (e.g., *FFT*) is paired with a second benchmark chosen randomly in each of the 20 runs. Compared to the no-security baseline (13.8 cycles), AES-128 increases average delay by over 19x (266.5 cycles), while our

TABLE III: Performance comparison for 8x8: 2 benchmarks

Benchmark	Delay: No Security		Delay: AES-128		Delay: Proposed	
	Avg	Max	Avg	Max	Avg	Max
FFT + 1	14.1	60	263.9	658	40.2	95
OCEAN + 1	14.9	50	261.7	654	39.9	95
RADIX + 1	15.1	57	263.1	640	38.7	97
FMM + 1	11.3	57	272.4	652	39.0	91
LU + 1	14.3	50	262.6	654	39.4	95
BARNEs + 1	12.2	56	272.2	665	39.2	95
black + 1	14.7	54	265.3	654	40.1	105
Average	13.8	60	266.5	665	39.5	105

proposed method results in only a 2.9x increase (39.5 cycles), confirming its efficiency under multi-application workloads.

##### B. Discussion

Table IV shows the eavesdropping probability under one and two-router threat models for both the baseline and our approach. The probabilities were computed by evaluating all possible permutations source-destination pairs and malicious router placements; a scenario was marked as an eavesdropping case if any malicious router lies on the packet path. In the case of a single malicious router, our method reduces the eavesdropping probability to 0% for both mesh sizes (e.g., from 6.85% to 0% in 8x8). Even under the more pessimistic model with two malicious routers, our method limits eavesdropping probability to just 0.47%. Compared to the AES-128 CTR approach, our AONT-based method achieves an approximate 79% area reduction in a 64-node NoC, based on gate-equivalent (GE) estimates synthesized using a 28nm standard cell library. In contrast to AES, our approach also eliminates the overhead of key sharing and secure key storage, as it does not require a pre-shared key between the source and destination.

TABLE IV: Eavesdropping probabilities for different scenarios

NoC Size	Threat Model	Defense	Eavesdropping Probability
4 x 4	1 malicious router	No defense	10.71%
	1 malicious router	Our approach	0%
8 x 8	2 malicious routers	No defense	41.76%
	2 malicious routers	Our approach	4.41%
8 x 8	1 malicious router	No defense	6.85%
	1 malicious router	Our approach	0%
8 x 8	2 malicious routers	No defense	13.21%
	2 malicious routers	Our approach	0.47%

#### V. CONCLUSION

This paper presented a lightweight confidentiality-preserving framework for secure on-chip communication in NoC architectures. By integrating a quasi-group-based AONT with disjoint multi-path routing, our approach ensures that intermediate routers cannot reconstruct the original message without access to all packet blocks. Experimental results on realistic workloads confirms that our approach provides confidentiality guarantees with 7.3 times reduction in performance overhead compared to AES, highlighting its effectiveness in defending against eavesdropping attacks.

## REFERENCES

- [1] H. Weerasena *et al.*, “Security of electrical, optical, and wireless on-chip interconnects: A survey,” *ACM TODAES*, vol. 29, no. 2, pp. 1–41, 2024.
- [2] ———, “Lightweight encryption using chaffing and winnowing with all-or-nothing transform for network-on-chip architectures,” in *HOST*, 2021.
- [3] S. I. Marnas *et al.*, “All-or-nothing transforms using quasigroups,” in *Proc. 1st Balkan Conference in Informatics*, 2003, pp. 183–191.
- [4] N. Binkert *et al.*, “The gem5 simulator,” *SIGARCH CA News*, 2011.
- [5] V. Catania *et al.*, “Cycle-accurate network on chip simulation with noxim,” *ACM TOMACS*, vol. 27, no. 1, pp. 1–25, 2016.
- [6] S. C. Woo *et al.*, “The splash-2 programs: Characterization and methodological considerations,” *CA News*, vol. 23, no. 2, pp. 24–36, 1995.
- [7] C. Bienia *et al.*, “The parsec benchmark suite: Characterization and architectural implications,” in *PACT*, 2008, pp. 72–81.